*Optica Applicata, Vol. XVIII, No. 3, 1988*

# Birefringence measurement in optical silica fibres *

W. URBAŃCZYK, K. PIETRASZKIEWICZ

Institute of Physics, Technical University of Wrocław, Wybrzeże Wyspiańskiego 27, 50–370 Wrocław, Poland.

A photometric method of birefringence measurement employing the polarization state modulation of the illuminating beam has been presented. Two detection channels are used. In the first one, the amplitude of the first harmonic of the light intensity incident on the photodetector is measured, while in the other one – the average value of this intensity. The quotient of both quantities is sent to the memory as a result of measurement. The achieved measurement sensitivity is of order of 1 Å. The application of the rotational half-wave plate rendered it possible to perform a simple calibration of the measuring system. As it was shown by the detailed analysis of systematic errors, the calibration procedure minimizes also the influence of the defects of both the manufacturing and the alignment of separate elements of the system on the final measurement error.

## 1. Introduction

Optical fibres of silica show usually small birefringence. This is caused by the residual internal stresses (resulting, in turn, from the differences in thermal expansion of the cladding and the core, respectively), and also by the difference in cooling rate of the external and internal zones of the fibre in drawing process. If a birefringent fibre is illuminated perpendicularly to its axis of symmetry (Fig. 1) by the plane wave

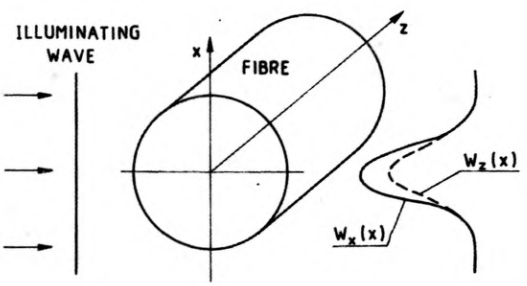


Fig. 1. Splitting the illuminating plane wave after the passage through the birefringence fibre

linearly polarized with azimuth at 45° to the symmetry axis of the fibre two wavefronts of linear polarizations $W_x(x)$ and $W_z(x)$ consistent with the directions of $x$, $z$ axes are observed in the space behind the fibre, respectively. The appearing

* This work was carried out under the Research Project RR I.02.

difference of wavefronts

$$R(x) = W_x(x) - W_z(x) \tag{1}$$

is connected merely with the fibre birefringence. The measurement of $R(x)$ enables the calculation of the cylindrical components of the internal stress $\sigma_r(r)$, $\sigma_\theta(r)$, $\sigma_z(r)$ of the fibre as well as anisotropy of the refractive index $n_r(r) - n_z(r)$, $n_\theta(r) - n_z(r)$, $n_r(r) - n_\theta(r)$, see [1]–[4], for example. The internal stresses influence both mechanical and chemical resistance of the fibre while anisotropy of the refractive index may worsen its transmission parameters. For these reasons the measurement of the wavefront differences $R(x)$ evoked by the phenomenon of fibre birefringence is the subject of interest of technologists. In the present paper the method of birefringence measurement used by the authors is described.

## 2. Methods of birefringence measurement by using the modulation of the polarization state

There are many known ways of measurement of birefringence while the most traditional Senarmonte and Babinet–Soleil compensation methods are still in common use. However, in the course of the last 25 years the new methods have appeared. These methods employ the technique of polarization state modulation of the illuminating light beam as well as the homodyne detection of the first harmonic component intensity. For the sake of clarity it will be useful to review the more important achievements in the modulation techniques.

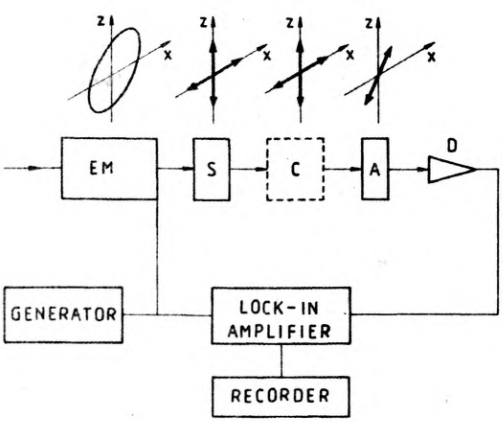


Fig. 2. Block scheme of a typical system for measuring the birefringence with the application of the polarization state modulation technique

The block scheme of a typical measuring system is shown in Fig. 2. It is composed of the following elements: modulator of ellipticity EM, examined sample S, compensator C (only for the methods with the null detection), analyser A, and photodetector D. The modulator EM introduces sinusoidal modulation of the illuminating beam ellipticity for its constant azimuth of polarization equal to 45°

with respect to the $x$ axis

$$v(t) = v_1 \sin \omega t \tag{2}$$

where $v_1$ and $\omega$ denote the amplitude and frequency of modulation, respectively. As a matter of fact, this means that it is the phase difference between the components of wave of polarization $x$ and $z$, that is modulated. The azimuths of the faster axes of the examined samples and that of the compensator C are identical. Thus, the static phase shift introduced by these elements is added to the alternating phase shift introduced by the modulator. Therefore, the light intensity after passage through the analyser A of 45° azimuth with respect to the $x$ axis is equal to

$$I(t) = I_0 [1 - \cos(\varphi_S + \varphi_C + v_1 \sin \omega t)], \tag{3a}$$

and after being expanded into series of harmonic components it takes the form

$$I(t) = I_0 [1 - J_0(v_1) \cos(\varphi_S + \varphi_C) + 2 \sin(\varphi_S + \varphi_C) \times \sum_{n=\text{odd}} J_n(v)_1 \sin(n\omega t) - 2 \cos(\varphi_S + \varphi_C) \sum_{n=\text{even}} J_n(v_1) \cos(n\omega t)] \tag{3b}$$

where $J_i$ are the Bessel functions of first kind. The signal from the detector D is proportional to $I(t)$. Due to the application of homodyne detection with the reference signal of frequency $\omega$ only first harmonic is selected from $I(t)$. This contains the information of resultant phase shift

$$I_\omega = I_0 J_1(v_1) \sin(\varphi_S + \varphi_C). \tag{4}$$

In general, two ways of measurement may be distinguished: the null detection technique and the photometric technique. As far as null detection technique is concerned the measured phase shift $\varphi_S$ is balanced by the phase shift $\varphi_C$ introduced by the compensator. The equality $\varphi_S = -\varphi_C$ occurs when the first harmonic of $I_\omega$ is equal to zero. The compensators applied to the measurement may be either of mechanical type, for example those of Senarmonte, Babinet–Soleil or electrooptic type like Pockels or Faraday cells, for instance. Takasaki was probably the first who proposed to use the modulation of the state of polarization to the measurements of birefringence as well as to ellipsometric and polarimetric measurements [5]–[7]. He employed KDP crystal as a modulator while the detection of null he realized with the help of Senarmonte compensator. Later on, there appeared many modifications of this method. ALLEN et al. [8], [9] and then MICHERON and BISMUTH [10] suggested the usage of electrooptic compensator based on ADP while SERREZE and GOLDNER [11] used the Babinet–Soleil compensator.

The photometric method was applied for the first time by JASPERSON et al. [12] to ellipsometric measurements. Its feature is a parallel homodyne detection of the first and the second harmonics of intensity

$$\begin{aligned} I_\omega &= I_0 J_1(v_1) \sin \varphi_S, \\ I_{2\omega} &= I_0 J_2(v_1) \cos \varphi_S. \end{aligned} \tag{5}$$

The pase shift introduced by the examined sample is indicated by the ratio $I_{2\omega}/I_{\omega}$ being proportional to tan $\varphi_S$. Clearly, no compensation is needed in this case, which makes the measurement much faster. In order to shorten the measurement time, Jasperson applied also for the first time an elastooptic modulator assuring the modulation frequency of order of dozens of MHz. The above idea was used later by several authors for the measurement of birefringence (e.g., MODINE et al. [13], [14], BENARD et al. [15], SHINDO et al. [16]). Both measuring methods are characterized by very high sensitivity of order of 1 Å or less. The photometric methods, though much faster, show lesser dynamics of measurement, which is connected with (usually) low dynamics of homodyne amplifiers.

The measuring method suggested in this paper may be classified as belonging to the group of photometric methods. The two-channel detection was applied. In the first channel the first harmonic $I_{\omega}$ is measured, while in the other – the average $\langle |I(t)-\langle I(t)\rangle| \rangle$, where $\langle \ldots \rangle$ denotes averaging in time. The result of measurement is the ratio $S(\varphi_S) = I_{\omega}/\langle |I(t)-\langle I(t)\rangle| \rangle$. The phase shift introduced by the examined fibre is calculated on the basis of the measured ratio $S(\varphi_S)$ with the help of the calibration curve. The calibration of the measuring system is carried out by using a modulator of ellipticity enabling the introduction of the controlled phase shift $v_0$

$$v(t) = v_0 + v_1 \sin \omega t. \tag{6}$$

As shown in Sect. 4 the calibration procedure minimizes also the systematic errors of measurement.

## 3. Description of measuring system

The diagram of the measuring system is shown in Figure 3. Due to significant simplification of the formulae in the analysis of errors carried out in Sect. 4 the azimuths of all the elements of the system are referred to the diagonal of the $(x, z)$

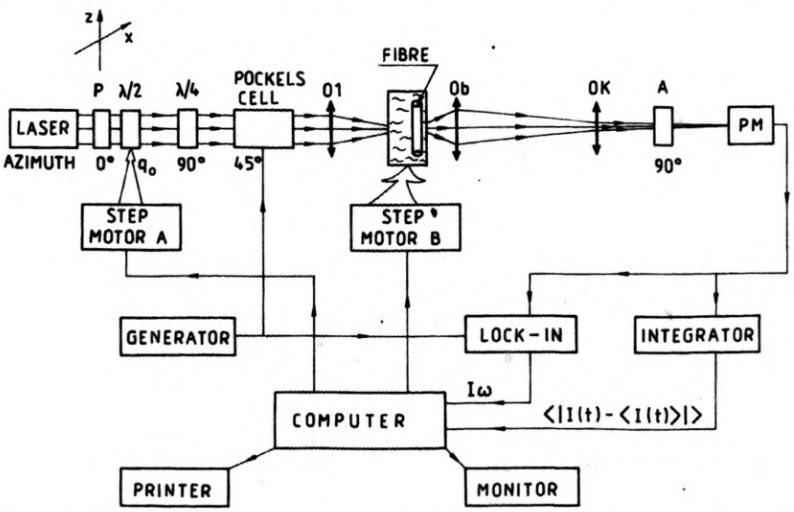


Fig. 3. Diagram of the system for measuring of the birefringence of the optical fibres

coordinate system. A 5 mW He-Ne laser is used as the light source. The ellipticity modulator is composed of the following elements: polarizer P, half-wave plate $\lambda/2$ being turned around the optical axis by the stepping motor A, quarter-wave plate $\lambda/4$ of azimuth of the faster axis equal to 90°, and the Pockels cell made of KDP of azimuth 45°. The frequency of modulation is equal to 7 kHz and amplitude – 90°. The rotational half-wave plate enables the introduction of the controlled phase shift $v_0$ while the following equality holds

$$v_0 = 4q_0 \tag{7}$$

where $q_0$ is the azimuth of the half-wave plate. During the measurement the azimuth of the half-wave plate is equal to 0°. The modulated beam passes through the objective O1 and illuminates the examined fibre which is positioned vertically (azimuth equal to 45°) and immersed in the liquid of refractive index matched to that of the cladding. The cuvette with the fibre is shifted across the beam by a stepping motor B of minimal step equal to 1 μm. The microscope objective of 10× magnification and the projection ocular (8×) form an enlarged image of the fibre in the plane of scanning slit of the photomultiplier. In front of the slit an analyser A of 90° transmission azimuth is located. Thus, the intensity of the light falling on the photomultiplier during the measurement and calibration may be described by the formulae:

$$\begin{aligned} I^{\mathrm{m}}(t) &= I_0[1-\cos(\varphi_{\mathrm{S}}+v_1\sin\omega t)], \\ I^{\mathrm{C}}(t) &= I_0[1-\cos(4q_0+v_1\sin\omega t)], \end{aligned} \tag{8}$$

respectively. As a result of measurement (calibration) the ratio

$$S(\varphi_{\mathrm{S}}) = \frac{I_\omega}{\langle |I(t)-\langle I(t)\rangle|\rangle} \tag{9}$$

is taken. Both signals, i.e., $I_\omega$ and $\langle |I(t)-\langle I(t)\rangle|\rangle$ are sent to the memory via two independent channels of detection. The resolution of both channels is 12 bits while the processing time is equal to 10 ms. The first harmonic is selected from $I(t)$ by a homodyne amplifier. The average $\langle |I(t)-\langle I(t)\rangle|\rangle$ is obtained after a very simple electronic processing of the signal $I(t)$, Fig. 4. If condition $\varphi_{\mathrm{S}} \ll v_1$ is fulfilled the result of averaging is practically independent of the value of the measured phase shift. Therefore, for great depths of modulation the course of the function $S(\varphi_{\mathrm{S}})$ is close to that of $\sin(\varphi_{\mathrm{S}})$, see Fig. 5, where the calculated dependence $S(\varphi_{\mathrm{S}})$ is shown for different $v_1$.

Before starting each measurement the system may be calibrated. This is done in such a way that stepping motor A changes the azimuth of the half-wave plate $q_0$ and after performing each step the quotient $S(4q_0)$ is measured. Typically, 20 points of calibration for the whole measurement range were used. The knowledge of calibration curve $S(4q_0)$ enables the calculation of the phase shift $\varphi_{\mathrm{S}}$ introduced by the examined fibre if the measured quotient $S(\varphi_{\mathrm{S}})$ is known.

Since the problem of uniqueness must be taken account of, the maximal measurement range is dependent upon the modulation depth (Fig. 5). For the depth

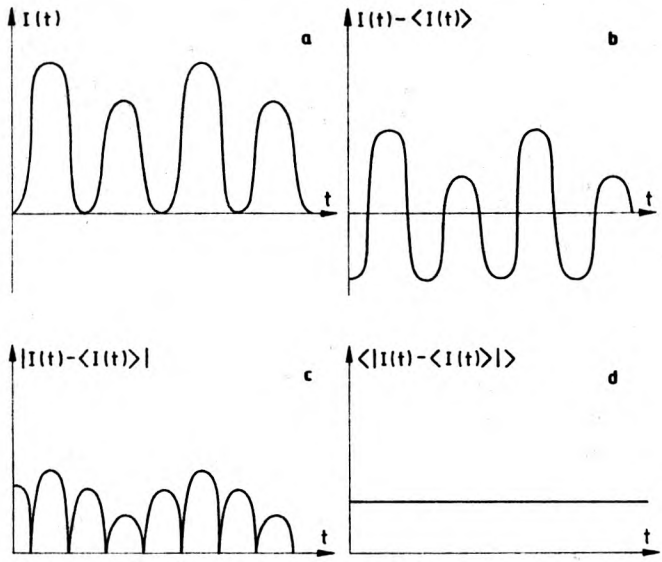


Fig. 4. Particular phases (**a-d**) of the electronic processing of the input signal for the detection channel with integrator

of modulation equal to 90°, as applied by the authors, the measurement range amounts to $\pm 97$ nm (55°).

The examined fibre is shifted step by step with respect to the immobile slit of the photomultiplier. At each scanning point 6 measurements are made and their average value is a final result. The time constant of the homodyne nanovoltmeter equal to

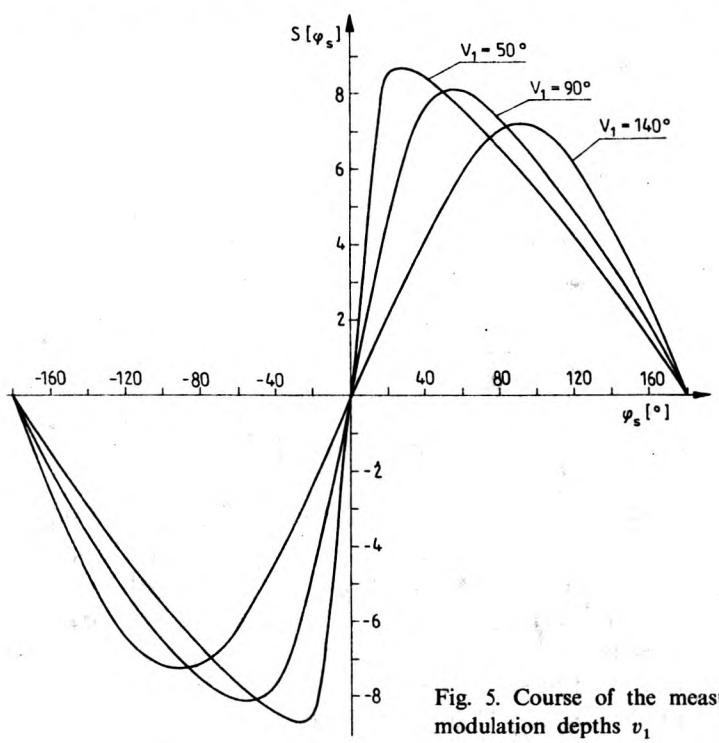


Fig. 5. Course of the measured signal $S(\varphi_S)$ for different modulation depths $v_1$

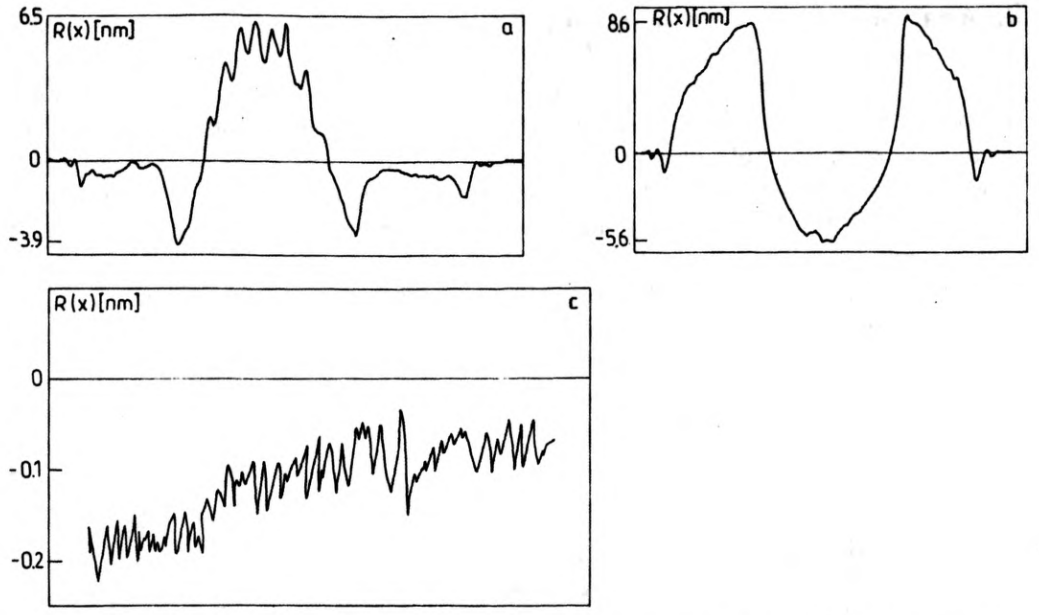


Fig. 6. Exemplified results of the measurement for two different silica fibres. **a** – fibre of graded-index profile, **b** – fibre of step-index profile, **c** – noise level of the measuring system. In the vertical axis the differences of the optical paths $R(x) = \frac{\lambda}{2\pi}\varphi_s(x)$ (in nm) are shown ($\lambda$ – illumination light wavelength). The local maxima observed in the case **a** result from the step character of the refractive index profile

0.3 s makes it sure that the measurement time at one scanning point is 2 s. In Figures **6a, b** the exemplified results of measurements of the optical path difference are shown for fibre of both the step-index and the graded-index profiles. Besides, in Fig. 6**c** the noise level of the system, measured under conditions identical with those for the fibre measurements has been illustrated. Both the drift of zero (connected most probably with the instability of electronic systems or temperature changes in the Pockels cell) and the short time noise do not exceed the value $\pm 1$ Å. Thus, this number may be accepted as representing the sensitivity of the measuring system. The error of measurement estimated to be equal to 5% is connected with the accuracy of both the channels of detection, i.e., homodyne nanovoltmeter (3%) and the integrating system (2%). As it will be shown in the next section, the measurement method offers high resistivity to systematic errors connected with the production and alignment errors of particular elements of the system. Besides, due to the fact that the quotient of two components of the same signal $I(t)$ is the result of measurement the errors resulting from the following are minimized:

- instability of laser power,
- instability of feeding voltage of the photomultiplier,
- impurities in the examined fibre,
- errors of fibre focusing which in the case of coherent light cause appearance of the corresponding changes of intensity in the image plane.

## 4. Analysis of systematic errors

The causes for the systematic errors in the measuring systems may be errors made during both the production of particular elements, and their alignment and also the residual birefringence of optical elements such as the lenses and walls of the cuvette in which the fibre is located. The analysis will be carried out with the use of Müller matrix description. At the beginning, let us assume that all the elements of the system: analyser A, half-wave plate $\lambda/2$, quarter-wave plate $\lambda/4$, Pockels cell, examined fibre, and polarizer P are produced and aligned perfectly. Then, they may be described by the following Müller matrices [16]:

$$\hat{M}_{\mathrm{P}} = \frac{1}{2}\begin{bmatrix} 1, & 1, & 0, & 0 \\ 1, & 1, & 0, & 0 \\ 0, & 0, & 0, & 0 \\ 0, & 0, & 0, & 0 \end{bmatrix},$$

$$\hat{M}_{\lambda/2} = \begin{bmatrix} 1, & 0, & 0, & 0 \\ 0, & \cos 4q_0, & \sin 4q_0, & 0 \\ 0, & \sin 4q_0, & -\cos 4q_0, & 0 \\ 0, & 0, & 0, & -1 \end{bmatrix},$$

$$\hat{M}_{\lambda/4} = \begin{bmatrix} 1, & 0, & 0, & 0 \\ 0, & 1, & 0, & 0 \\ 0, & 0, & 0, & -1 \\ 0, & 0, & 1, & 0 \end{bmatrix},$$

$$\hat{M}_{\mathrm{PC}} = \begin{bmatrix} 1, & 0, & 0, & 0 \\ 0, & \cos v(t), & 0, & \sin v(t) \\ 0, & 0 & 1, & 0 \\ 0, & \sin v(t), & 0, & \cos v(t) \end{bmatrix},$$

$$\hat{M}_{\mathrm{S}} = \begin{bmatrix} 1, & 0, & 0, & 0 \\ 0, & \cos \varphi_{\mathrm{S}}, & 0, & \sin \varphi_{\mathrm{S}}, \\ 0, & 0, & 1 & \\ 0, & \sin \varphi_{\mathrm{S}}, & 0, & \cos \varphi_{\mathrm{S}} \end{bmatrix},$$

$$\hat{M}_{\mathrm{A}} = \frac{1}{2}\begin{bmatrix} 1, & -1, & 0, & 0 \\ -1, & 1, & 0, & 0 \\ 0, & 0, & 0, & 0 \\ 0, & 0, & 0, & 0 \end{bmatrix} \tag{10}$$

where $v(t) = v_1 \sin \omega t$ is proportional to the voltage driving the Pockels cell. Due to the considerable simplification of the formulae the azimuth of all the elements of the system has been referred to the diagonal of the coordinate system $(x, z)$, see Fig. 3.

The intensity of the light incident on the photomultiplier PM may be calculated with the help of the Müller matrix. This is equal to the first component of the Stokes

vector $\hat{L}(t)$

$$\hat{L}(t) = \hat{M}_A \hat{M}_S \hat{M}_{PC}(t) \hat{M}_{\lambda/4} \hat{M}_{\lambda/2} \hat{M}_P \hat{L}_0 \tag{11}$$

where $\hat{L}_0$ represents the state of polarization of the beam entering the system (vertically polarized laser beam)

$$\hat{L}_0 = \begin{bmatrix} 1 \\ 1 \\ 0 \\ 0 \end{bmatrix}. \tag{12}$$

During the measurement and calibration of the system, intensity of the beam $I(t)$ is connected with the measured signal in the following ways:

$$S^m(\varphi_S) = \frac{I_\omega(\varphi_S)}{\langle |I(\varphi_S, t) - \langle I(\varphi_S, t)\rangle|\rangle}, \tag{13a}$$

$$S^c(4q_0) = \frac{I_\omega(4q_0)}{\langle |I(4q_0, t) - \langle I(4q_0, t)\rangle|\rangle}, \tag{13b}$$

respectively. For a perfect system the functions $S^m(\varphi_S)$ and $S^c(4q_0)$ are identically equal to each other

$$S^m(\varphi_S) \equiv S^c(4q_0). \tag{14}$$

The errors of alignment and production of the particular elements of the system may change the course of functions $S^m(\varphi_S)$ and $S^c(4q_0)$ in different ways. Consequently, for a nonideal system the relation (14) may not be fulfilled. This fact may cause the systematic errors of the measurements.

Let the vector $\vec{\Delta p} = (\Delta p_1, \Delta p_2, \ldots, \Delta p_n)$ describe the deviations of particular parameters of the system (such as azimuths and phase shifts) from the assumed values. The systematic error of the measurement for the nonideal system $\Delta\varphi_S$ may be then estimated on the basis of the following equation (Fig. 7):

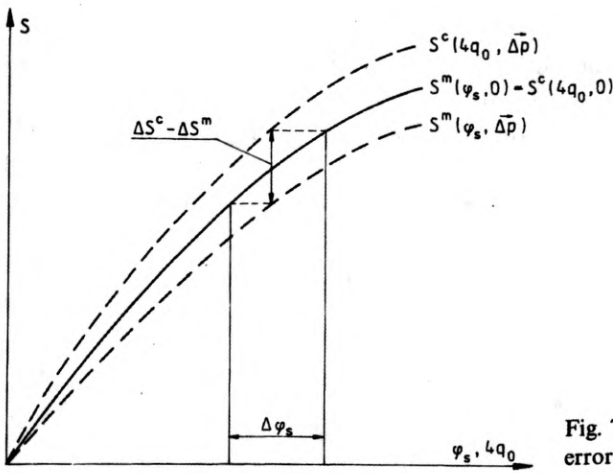


Fig. 7. To illustrate the cause of the systematic errors $\Delta\varphi_S$

$$S^{\mathrm{m}}(\varphi_{\mathrm{S}}, \vec{\Delta p}) = S^{\mathrm{c}}(4q_0 + \Delta\varphi_{\mathrm{S}}, \vec{\Delta p}). \tag{15}$$

From the approximation of the first order it follows that

$$\Delta\varphi_{\mathrm{S}} = \frac{\sum_i \left(\frac{\partial S^{\mathrm{m}}}{\partial p_i} - \frac{\partial S^{\mathrm{c}}}{\partial p_i}\right)\Delta p_i}{\frac{\partial S^{\mathrm{m}}}{\partial \varphi_{\mathrm{S}}}}. \tag{16}$$

The coefficients

$$q_i = \left(\frac{\partial S^{\mathrm{m}}}{\partial p_i} - \frac{\partial S^{\mathrm{c}}}{\partial p_i}\right) \Big/ \frac{\partial S^{\mathrm{m}}}{\partial \varphi_{\mathrm{S}}} \tag{17}$$

represent the coupling which exists in the first order approximation between the errors of particular elements of the system $\Delta p_i$ and the final measurement error $\Delta\varphi_{\mathrm{S}}$. In the following sections the coupling coefficients $q_i$ for particular elements of the system are determined.

### 4.1. Polarizers

Real polarizers applied in the measuring system may be described by the following Müller matrix [16]:

$$\hat{M}'_{\mathrm{P}} = \begin{bmatrix} k_0 + k_{90}, & C_2(k_0 - k_{90}), \\ C_2(k_0 - k_{90}), & C_2^2(k_0 + k_{90}) + 2S_2^2\sqrt{k_0 k_{90}}, \\ S_2(k_0 - k_{90}), & C_2 S_2(k_0 + k_{90}) - 2C_2 S_2\sqrt{k_0 k_{90}}, \\ 0, & 0, \end{bmatrix}$$

$$\begin{matrix} S_2(k_0 - k_{90}), & 0 \\ C_2 S_2(k_0 + k_{90}) - 2C_2 S_2\sqrt{k_0 k_{90}}, & 0 \\ S_2(k_0 + k_{90}) + 2C_2^2\sqrt{k_0 k_{90}}, & 0 \\ 0, & 0 \end{matrix} \Bigg] \tag{18}$$

where $C_2 = \cos 2\alpha$, $S_2 = \sin 2\alpha$ ($\alpha$ denotes the transmission azimuth), while $k_0$ and $k_{90}$ denote the coefficients of transmission of intensity for parallel and crossed polarizers, respectively. When replacing the matrices representing the polarizer $\hat{M}_{\mathrm{P}}$ and analyser $\hat{M}_{\mathrm{A}}$ in expression (11) by their respective nonperfect ($k_{90}/k_0 \neq 0$) counterparts it is possible to obtain, after some tedious transformations, the following expressions for the intensity of the light falling on the photomultiplier:

$$\begin{aligned} I^{\mathrm{m}}(t) &= I_0\left[(k_0 + k_{90})^2 - 2\sin 2\Delta p_{\mathrm{A}}(k_0 - k_{90})\sqrt{k_0 k_{90}}\right. \\ &\quad \left. -(k_0 - k_{90})^2 \cos(\varphi_{\mathrm{S}} + 2\Delta p_{\mathrm{P}} + v(t))\right], \\ I^{\mathrm{c}}(t) &= I_0\left[(k_0 + k_{90})^2 - 2\sin 2\Delta p_{\mathrm{A}}(k_0 - k_{90})\sqrt{k_0 k_{90}}\right. \\ &\quad \left. -(k_0 - k_{90})^2 \cos(4q_0 + 2\Delta p_{\mathrm{P}} + v(t))\right] \end{aligned} \tag{19}$$

during the calibration and measurements, respectively. In the above formulae $\Delta p_A$ and $\Delta p_P$ represent the alignment error of both the analyser and polarizer, respectively. The expressions for $I^m(t)$ and $I^c(t)$ are equal to each other if only $\varphi_S = 4q_0$, hence it follows that the poor quality ($k_{90}/k_0 \neq 0$) of the polarizers and their misalignment error cause no systematic errors of the measurements. Thus, the first order coupling coefficients as well as the coefficients of higher orders are equal to zero. It is only the signal to noise ratio which is decreased by the imperfections of polarizers and the errors of their alignment.

### 4.2. Object under test

Let us assume that the azimuth of the faster axis of the examined object (birefringent fibre) is equal to $45° + \Delta p_S$, where $\Delta p_S$ denotes the error of azimuth alignment. The Müller matrix of the examined fibre is thus given by

$$\hat{M}'_S = \begin{bmatrix} 1, & 0, & 0, & 0, \\ 0, & 1-2\sin^2\frac{\varphi_S}{2}\cos^2 2\Delta p_S, & -\sin^2\frac{\varphi_S}{2}\sin 4\Delta p_S, & \sin\varphi_S\cos 2\Delta p_S, \\ 0, & -\sin^2\frac{\varphi_S}{2}\sin 4\Delta p_S, & 1-2\sin^2\frac{\varphi_S}{2}\sin^2 2\Delta p_S, & -\sin\varphi_S\sin^2\Delta p_S \\ 0, & \sin\varphi_S\cos 2\Delta p_S, & \sin\varphi_S\sin 2\Delta p_S, & \cos\varphi_S \end{bmatrix}. \tag{20}$$

By substituting $\hat{M}'_S$ to the formula (11) and performing some tedious transformations it may be pointed out that the light intensity reaching the photomultiplier is equal to

$$\begin{aligned} I^m(t) &= I_0\left\{1-\cos v(t)\left[1-2\sin^2\frac{\varphi_S}{2}\cos^2 2\Delta p_S\right]+\sin v(t)\sin\varphi_S\cos 2\Delta p_S\right\}, \\ I^c(t) &= I_0\{1-\cos[v(t)+4q_0]\}. \end{aligned} \tag{21}$$

In the first order approximation, the functions $I^m(t, \Delta p_S)$ and $I^c(t, \Delta p_S)$ are identical. This means that the coupling coefficient of the first order connected with the alignment error of the examined object is equal to zero.

### 4.3. Pockels cell

Let us analyse the influence of the Pockels cell on the measurement accuracy. We assume that the azimuth of the Pockels cell is equal to $45° + \Delta p_C$, where $\Delta p_C$ denotes the alignment error. The Müller matrix of the Pockels cell will then be given by

$$\hat{M}'_{PC} = \begin{bmatrix} 1, & 0, & & \\ 0, & 1-2\sin^2\frac{v(t)}{2}\cos^2 2\Delta p_C, & & \\ 0, & -\sin^2\frac{v(t)}{2}\sin 4\Delta p_C, & & \\ 0, & \sin v(t)\cos 2\Delta p_C, & & \end{bmatrix}$$

$$\begin{bmatrix} 0, & 0 \\ -\sin^2\frac{v(t)}{2}\sin 4\Delta p_C, & -\sin v(t)\cos 2\Delta p_C \\ 1-2\sin^2\frac{v(t)}{2}\sin^2 2\Delta p_C, & -\sin v(t)\sin 2\Delta p_C \\ \sin v(t)\sin 2\Delta p_C, & \cos v(t) \end{bmatrix}. \quad (22)$$

After substituting $\hat{M}'_{PC}$ to the formula (11) we obtain:

$$I^m(t) = I_0\left[1+\sin v(t)\cos 2\Delta p_C \sin\varphi_S - \cos\varphi_S\left(1-2\sin^2\frac{v(t)}{2}\cos^2 2\Delta p_C\right)\right],$$

$$I^c(t) = I_0\left[1+\sin v(t)\cos 2\Delta p_C \sin 4q_0 - \cos 4q_0\left(1-2\sin^2\frac{v(t)}{2}\cos^2 2\Delta p_C\right)\right]. \quad (23)$$

The functions $I^m(t, \Delta p_C)$ and $I^c(t, \Delta p_C)$ are identical, which means that the error of alignment of the Pockels cell causes no systematic error of the measurement. The coupling coefficient of the first order as well as all the coefficients of higher orders are equal to zero.

### 4.4. Quarter-wave plate

Let us analyse the alignment and manufacturing defects of the quarter-wave plates on the measurement accuracy.

*i) Manufacturing defects*

Let us assume that the real phase shift introduced by the quarter-wave plate is equal to $90° + \Delta p_{\lambda/4}$ ($\Delta p_{\lambda/4}$ denotes the manufacturing defect). In this case, the Müller matrix of the quarter-wave plate is given by

$$\hat{M}'_{\lambda/4} = \begin{bmatrix} 1, & 0, & 0, & 0 \\ 0, & 1, & 0, & 0 \\ 0, & 0, & -\sin\Delta p_{\lambda/4}, & -\cos\Delta p_{\lambda/4} \\ 0, & 0, & \cos\Delta p_{\lambda/4}, & -\sin\Delta p_{\lambda/4} \end{bmatrix}. \quad (24)$$

After substituting $\hat{M}'_{\lambda/4}$ to the formula (11) and after performing laborious transformations the following is obtained:

$$\begin{aligned} I^{\mathrm{m}}(t) &= I_0[1-\cos(\varphi_{\mathrm{s}}-v(t))], \\ I^{\mathrm{c}}(t) &= I_0[1-\cos 4q_0\cos v(t)+\sin v(t)\sin 4q_0\cos \Delta p_{\lambda/4}. \end{aligned} \tag{25}$$

In the first order approximation, the functions $I^{\mathrm{m}}(t)$ and $I^{\mathrm{c}}(t, \Delta p_{\lambda/4})$ are identical, which means that the first order coupling coefficient connected with the manufacturing defect of quarter-wave plate is equal to zero.

*ii) Azimuth error*

Let us assume that the azimuth of the quarter-wave plate is equal to $90^+ + \Delta p_{\lambda/4}$, where $\Delta p_{\lambda/4}$ denotes now the alignment error. The Müller matrix for such a quarter-wave plate is given by

$$\hat{M}'_{\lambda/4} = \begin{bmatrix} 1, & 0, & 0, & 0 \\ 0, & \cos^2 2\Delta p_{\lambda/4}, & \sin 2\,\Delta p_{\lambda/4}\cos 2\Delta p_{\lambda/4}, & \sin 2\Delta p_{\lambda/4} \\ 0, & \sin 2\,\Delta p_{\lambda/4}\cos 2\Delta p_{\lambda/4}, & \sin^2 2\Delta p_{\lambda/4}, & -\cos 2\Delta p_{\lambda/4} \\ 0, & -\sin 2\Delta p_{\lambda/4}, & \cos 2\Delta p_{\lambda/4}, & 0 \end{bmatrix}. \tag{26}$$

After laborious rearrangements it may be shown that the light intensity falling on the detector during the measurement and the calibration is equal to

$$\begin{aligned} I^{\mathrm{m}}(t) &= I_0\{1-[\cos\varphi_{\mathrm{s}}\cos^2 2\Delta p_{\lambda/4}+\sin\varphi_{\mathrm{s}}\sin 2\Delta p_{\lambda/4}] \\ &\quad \times\cos v(t)+[\sin\varphi_{\mathrm{s}}\cos^2 2\Delta p_{\lambda/4}-\cos\varphi_{\mathrm{s}}\sin 2\Delta p_{\lambda/4}]\sin v(t)\}, \\ I^{\mathrm{c}}(t) &= I_0\{1-[\cos 4q_0\cos^2 2\Delta p_{\lambda/4}+\sin 4q_0\sin 2\Delta p_{\lambda/4}\cos 2\Delta p_{\lambda/4}]\cos v(t) \\ &\quad +[\sin 4q_0\cos 2\Delta p_{\lambda/4}-\cos 4q_0\sin 2\Delta p_{\lambda/4}]\sin v(t)\}, \end{aligned} \tag{27}$$

respectively. Similarly, as it was the case earlier in the first order approximation, the functions $I^{\mathrm{m}}(t, \Delta p_{\lambda/4})$ and $I^{\mathrm{c}}(t, \Delta p_{\lambda/4})$ are identical, which means that the partial derivatives $\partial S^{\mathrm{m}}/\partial p_{\lambda/4}$ and $\partial S^{\mathrm{c}}/\partial p_{\lambda/4}$ are equal to each other and the first order coupling coefficient disappears. Thus, in the first order approximation the error of quarter-wave plate azimuth causes no systematic errors of the measurements.

### 4.5. Half-wave plate

Let us assume that the real phase shift introduced by the half-wave plate is equal to $180° + \Delta p_{\lambda/2}$, where $\Delta p_{\lambda/2}$ is the manufacturing defect. The Müller matrix is given

then by

$$\hat{M}'_{\lambda/2} = \begin{bmatrix} 1, & 0, & 0 & 0 \\ 0, & 1-2\cos^2\frac{\Delta p_{\lambda/2}}{2}\sin^2 2q_0, & \cos^2\frac{\Delta p_{\lambda/2}}{2}\sin 4q_0, & \sin\Delta p_{\lambda/2}\sin 2q_0 \\ 0, & \cos^2\frac{\Delta p_{\lambda/2}}{2}\sin 4q_0, & 1-2\cos^2\frac{\Delta p_{\lambda/2}}{2}\cos^2 2q_0, & -\sin\Delta p_{\lambda/2}\cos 2q_0 \\ 0, & -\sin\Delta p_{\lambda/2}\sin 2q_0, & \sin\Delta p_{\lambda/2}\cos 2q_0, & -\cos\Delta p_{\lambda/2} \end{bmatrix}. \tag{28}$$

After substituting $\hat{M}'_{\lambda/2}$ to expression (11) we find the intensity of the light incident on the photomultiplier during measurement and calibration

$$I^{m}(t) = I_0[1-\cos(v(t)+\varphi_s)],$$
$$I^{c}(t) = I_0\left[1-\left(1-2\cos^2\frac{\Delta p_{\lambda/2}}{2}\sin^2 2q_0\right)\cos v(t)+\cos^2\frac{\Delta p_{\lambda/2}}{2}\sin 4q_0\sin v(t)\right]. \tag{29}$$

In the first order approximation both functions are identical, which means that the coupling coefficient connected with the manufacturing defect of the half-wave plate is equal to zero.

### 4.6. Optical window

The optical elements of the measuring system such as walls of the cuvette and the lenses have usually some residual birefringence evoked by the stress. We shall analyse the influence of the residual birefringence of the optical elements located in front of and behind the examined objects (input and output optical windows) on the errors of measurement.

It may be easily shown that the birefringence of the output window of the system has no influence on the measurement accuracy. This modifies the state of polarization of the beam in the space between the fibre and the analyser, which may change the final intensity of the beam. However, these changes remain identical during both the measurement and the calibration of the system, and for these reasons cause no errors of measurements.

In order to estimate the influence of the residual birefringence of the input window of the system on the measurement error, let us assume that the birefringence is uniform across the whole cross-section of the beam. The input window may then

be described by the Müller matrix $\hat{M}_W$ [16]. The Stokes vector for the light emerging from the system will now be equal to

$$\hat{L}(t) = \hat{M}_A \hat{M}_S \hat{M}_W \hat{M}_{PC}(t) \hat{M}_{\lambda/4} \hat{M}_{\lambda/2} \hat{M}_P \hat{L}_0 \tag{30}$$

where – if compared with the formula (11) – the matrix $\hat{M}_W$ has been added, which represents the input window of the system. After tedious transformations it may be pointed out that the intensity during the measurement and calibration is equal to

$$\begin{aligned} I^m(t) &= I_0 \{1 - \cos v(t) [M^W_{24} \sin \varphi_S + M^W_{22} \cos \varphi_S] \\ &\quad + \sin v(t) [M^W_{44} \sin \varphi_S - M^W_{24} \cos \varphi_S]\}, \\ I^c(t) &= I_0 \{1 - \cos v(t) [M^W_{24} \sin 4q_0 + M^W_{22} \cos 4q_0] \\ &\quad + \sin v(t) [M^W_{22} \sin 4q_0 - M^W_{24} \cos 4q_0]\}, \end{aligned} \tag{31}$$

respectively, where $M^W_{ij}$ are the elements of the $\hat{M}_W$ Müller matrix:

$$\begin{aligned} M^W_{24} &= -\sin 2\alpha \sin \Delta p_W, \\ M^W_{22} &= \sin^2 \frac{\Delta p_W}{2} \cos 4\alpha + \cos^2 \frac{\Delta p_W}{2}, \\ M^W_{44} &= 2\cos^2 \frac{\Delta p_W}{2} - 1. \end{aligned} \tag{32}$$

In the above formulae $\alpha$ and $\Delta p_W$ denote the azimuth of the faster axis and the phase delay introduced by the residual birefringence of the window, respectively. In the first order approximation the expressions for $I^m(t)$ and $I^c(t)$ are identical, which means that $\partial S^m / \partial p_W = \partial S^c / \partial p_W$. Thus, the first order coupling coefficient connected with the birefringence of input window of the system is also equal to zero.

## 5. Summarizing remarks

As pointed out by the above analysis, the proposed method of birefringence measurement in the silica optical fibres is characterized by low susceptibility to the systematic errors connected with the alignment and manufacturing accuracy of the particular element of the system. In the first order approximation, all the coupling coefficients are equal to zero. This fact is mainly due to the application of the calibration procedure of measurement system.

The proposed system requires much simpler, and therefore less expensive electronics if compared with traditional photometric method consisting in measuring the first and the second harmonic of the intensity. The homodyne detection of the second harmonic has been replaced by the averaging of the input signal which is much simpler to perform. Some shortcoming of the method is the limited measurement range $\pm 97$ nm. However, in the case of optical silica fibres as well as in

many other measurement applications this fact is of no significance since the greatest optical path differences observed by us for fibres of that kind were comprised in the $\pm 10$ nm interval.

*Acknowledgements* – The examined fibres were provided by the Institute of Chemistry, Maria Skłodowska–Curie University, Lublin, Poland.

## References

[1] CHU P. L., WHITBREAD T. W., Appl. Opt. **21** (1982), 4241.
[2] SCHERER G. W., Appl. Opt. **19** (1980), 2000.
[3] URBAŃCZYK W., PIETRASZKIEWICZ K., *Measurement of stress induced anisotropy in fibre preform. Modification of dynamic spatial filtering technique.* Appl. Opt., accepted for publication.
[4] BACHMANN P. K., HERMANN W., WEHR H., Appl. Opt. **25** (1986), 1093.
[5] TAKASAKI H., J. Opt. Soc. Am. **51** (1961), 462.
[6] TAKASAKI H., J. Opt. Soc. Am. **51** (1961), 463.
[7] TAKASAKI H., Appl. Opt. 56 (1966), 759.
[8] ALLEN R. D., BRAULT J. W., ZEH R. M., [in] *Advances in Optical and Electron Microscopy*, Academic Press, New York 1966, Vol. 1, pp. 77–114.
[9] ALLEN R. D., BRAULT J. W., MOORE R. D., J. Cell. Biol. **18** (1962), 223.
[10] MICHERON F., BISMUTH G., Rev. Sci. Instrum. **43** (1972), 292.
[11] SERREZE H. B., GOLDNER R. B., Rev. Sci. Instrum. **45** (1974), 1613.
[12] JASPERSON S. N., BURGE D. K., O'HANDLY R. C., Surface Sci. **37** (1973), 548.
[13] MODINE F. A., MAJOR R. W., SONDER E., Appl. Opt. **14** (1975), 757.
[14] MODINE F. A., MAJOR R. W., Appl. Opt. **14** (1975), 761.
[15] BENARD D. J., WALKER W. C., Rev. Sci. Instrum. **47** (1976), 122.
[16] SHINDO Y., HANABUSA H., Polym. Commun. 24 (1983), 240.
[17] SHURCLIFF W. A., BALLARD S. S., *Polarized Light*, Van Nostran, Princeton 1964.

*Received March 16, 1988*

## Метод измерения двойного лучепреломления кварцевых оптических волокон

Представлено фотометрический метод измерения двойного лучепреломления с использованием модуляции состояния поляризации осветительного пучка. Применено два канала детектирования. Первым является измеренная амплитуда первой гармонической силы света падающего на фотодетектор, другим же – средняя этой силы. В виде результата измерения запоминается частное обоих величин. Достигнуто чувствительность измерения ряда 1 Å. Применение вращательной полволновой пластинки дало возможность несложной калибровки измирительной системы. Как доказал подробный анализ систематических ошибок, процедура калибровки минимизирует также влияние ошибок воспроизведения и заключения очередных элементов системы на точность измерения.